Swap Mott transition in multicomponent fermion systems

Duc-Anh Le [1] Thanh-Mai Thi Tran [2] and Minh-Tien Tran [2]

[1]*Faculty of Physics, Hanoi National University of Education, Hanoi 11300, Vietnam*
[2]*Institute of Physics, Vietnam Academy of Science and Technology, Hanoi 10072, Vietnam*

Metal-insulator transitions in an asymmetric three-component Falicov-Kimball model are investigated within the two-site dynamical mean field theory. The model is obtained from the symmetry breaking of the $SU(3)$ Hubbard model by imbalanced masses and nonequal local interactions of particle components. The Mott transitions are classified by the change in the number of distinct kinds of doublons across the transition. We observe a different Mott transition between partially localized states in which the particle components (flavors), which form the doublons, are swapped with each other but the number of distinct kinds of doublons is unchanged across the transition. The swap Mott transition occurs as a result of the competition between the Brinkman-Rice and the Falicov-Kimball localizations and the mass imbalance of the mobile particles.

DOI: 10.1103/PhysRevB.109.115105

I. INTRODUCTION

The Mott transition is one of the fascinating problems in condensed matter physics due to its striking manifestation of many-body correlation effects [1]. A strong repulsive interaction between electrons prevents doublon formation (i.e., a pair of electrons occupying the same lattice site), and that leads to electron localization when the electron density is commensurate with the number of lattice sites. This is an intuitive and key feature of the Brinkman-Rice scenario of the Mott transition [2]. Within the Brinkman-Rice scenario, both the mass renormalization and the doublons are suppressed in the Mott insulator. Therefore, one can use mass renormalization or the doublons to detect the Mott transition. However, in multicomponent (flavor) fermion systems, where the degeneracy (the number of flavors) of the charge carriers is larger than two, different Mott insulating states can exist [3–9]. For example, in three-component fermion systems, so-called collective and paired Mott insulators can occur [3–7]. The collective Mott insulator is characterized by the localization of particles of any component at each lattice site, and all doublons are suppressed [3]. In the paired Mott insulator, the doublons formed by particles of two different components and the particles of the remaining component are localized [4]. In both collective and paired Mott insulators, the mass renormalizations of all particle components vanish, and they can no longer distinguish these Mott insulating states [3–7]. Therefore, in multicomponent fermion systems, the Mott transition is more suitably determined by using doublons rather than using mass renormalization. Experiments have indeed used doublons to detect the Mott transition in optical lattices [10,11].

In N-component fermion systems, the number of distinct kinds of doublons is $N_d = N(N-1)/2$. Different Mott insulators may occur when some kinds of doublons are suppressed while others occur. Such states can be found in the partial localization of electrons and orbital-selective or paired Mott insulators [12–18]. One can use the number of distinct kinds of doublons to classify the Mott insulators in multicomponent fermion systems. For example, in three-component fermion systems, $N = 3$, and there are three distinct kinds of doublons, $N_d = 3$. The collective Mott insulator is characterized by $N_d = 0$ [3]. The paired Mott insulator is characterized by $N_d = 1$ [4]. The metallic state can also be classified by $N_d = 3$. The Mott transition, therefore, can be classified by the change in the number of distinct kinds of doublons $\Delta N_d \equiv N_{d1} - N_{d2}$ across the transition, where N_{d1} and N_{d2} are the numbers of distinct kinds of doublons in phase 1 and phase 2 of the phase transition. In electron systems with $N = 2$, there is only one kind of doublon, and the Mott transition is characterized by $\Delta N_d = 1$. The partial localization in $5f$ heavy fermion compounds can also be characterized by $\Delta N_d = 1$ [12–14]. The orbital-selective Mott transition of degenerate $4d$ systems can occur with $\Delta N_d = 1$ [15,16]. In the three-component Hubbard model, the collective Mott transition is characterized by $\Delta N_d = 3$, while the paired one occurs with $\Delta N_d = 2$ (for their illustrations see Fig. 1) [3–7]. So far, all well-known Mott transitions occur with $\Delta N_d \neq 0$; i.e., the number of distinct kinds of doublons changes across the transitions. However, there is still another possibility of the Mott transition which occurs with $\Delta N_d = 0$. In that Mott transition both phases have the same number of distinct kinds of doublons, but different kinds of doublons occur in each phase. Across the transition the particle components that form the doublons are swapped with each other. We call this *swap Mott transition*. The swap Mott transition is actually the phase transition from one partially localized state to another one with different kinds of doublons while the number of distinct kinds of doublons remains the same.

In the present paper, we will show the possibility of the swap Mott transition in minimal multicomponent fermion models. With the achievement of the ultracold technique, experiments can establish optical lattices of neutral atoms and simulate quantum fermion lattice models [19,20]. Optical lattices allow us to flexibly control and tune the model parameters. In particular, the particle degeneracy can be large
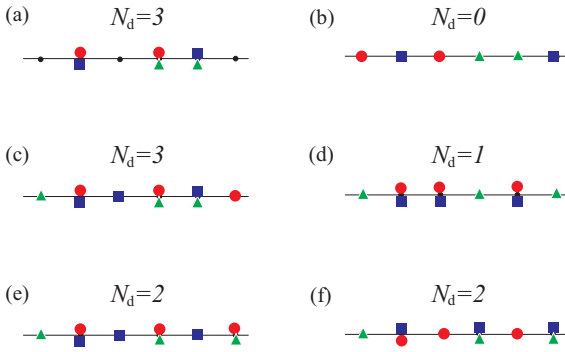
FIG. 1. Schematic illustration of Mott transitions in three-component fermion systems. Circles, squares, and triangles schematically represent fermions with different components (flavors). There are only three possible distinct kinds of doublons: circle-square, square-triangle, and triangle-circle ($N_d = 3$). The first row illustrates the Mott transition from (a) a metallic state with $N_d = 3$ to (b) a collective Mott insulator with $N_d = 0$ at one third filling. In (b), the local Coulomb interaction prevents the occupancy of two particles at the same site; thus, the particles cannot move in the lattice and form the Mott insulating state. The second row illustrates the Mott transition from (c) a metallic state with $N_d = 3$ to (d) a paired Mott insulator with $N_d = 1$ at half filling. In (d), the doublons of the "circle" and "square" components and the particles of "triangle" component are localized and form the paired Mott insulator. The third row illustrates the swap Mott transition from (e) a partially localized state with $N_d = 2$ to (f) another partially localized state with $N_d = 2$. In (e), two kinds of doublons, circle-square and circle-triangle, are localized, while in (f), two other kinds of doublons, square-circle and square-triangle, are localized. Across the transition, the circle component and the square component are swapped with each other in the doublon formation.

and odd, which does not have an obvious counterpart in crystalline lattices. Correlated two-component models, i.e., the standard Hubbard model and its variations, exhibit the Mott transition, which always occurs with $\Delta N_d = 1$. The Mott transition also occurs in the three-component Hubbard model [3–9]. However, the three-component Hubbard model with $SU(3)$ symmetry exhibits only the collective Mott transition with $\Delta N_d = 3$ at commensurate fillings [3,4]. When $SU(3)$ symmetry is broken by either the local interactions or the hopping, the three-component Hubbard model also additionally realizes the Mott transitions with $\Delta N_d = 1, 2$ at half filling [4–6]. We will show with further symmetry breaking by both hopping and local interactions that the three-component Hubbard model additionally exhibits a swap Mott transition with $\Delta N_d = 0$. This Mott transition has not previously been discussed. The simplest version of the symmetry breaking by both hopping and local interactions is an asymmetric three-component Falicov-Kimball model (FKM) with nonequal local interactions. Actually, the three-component FKM is a version of the $SU(2) \times U(1)$ symmetry of the three-component Hubbard model [5,6]. In this model, two components are identical and mobile, whereas the hopping term of the third component vanishes. The three-component FKM exhibits the Mott transition with $\Delta N_d = 3$ at commensurate fillings and partial localization Mott transitions with $\Delta N_d = 1, 2$ at half filling [5,6]. Its asymmetric version is

realized by allowing component dependence of the hopping term. This leads to a mass imbalance of the mobile components. We will apply the dynamical mean field theory (DMFT) to study the Mott transitions in the asymmetric FKM [21,22]. For simplicity, we will use the two-site version of the impurity solver in the DMFT [23]. This simplification usually loses the fine structure of the self-energy at intermediate energy scales, but it reduces the numerical calculations and still correctly captures the low- and high-frequency asymptotic behaviors of the self-energy and correctly describes the Mott transition within the Brinkman-Rice scenario [23]. In addition to the previously known Mott transitions [5,6], we find another Mott transition with $\Delta N_d = 0$ which is absent in the $SU(2) \times U(1)$ symmetry version of the three-component Hubbard model and the three-component FKM.

The structure of this paper is as follows. In Sec. II we present the asymmetric three-component FKM and the two-site DMFT for solving the proposed model. The numerical results and a discussion of the observed Mott transitions are presented in Sec. III. Finally, Sec. IV gives the conclusions.

II. ASYMMETRIC THREE-COMPONENT FALICOV-KIMBALL MODEL

In this section, we construct a lattice model of ultracold multicomponent atoms loaded into an optical lattice. Our purpose is to find a minimal model that exhibits a swap Mott transition. Since the correlated two-component fermion model does not exhibit any partial localization, we will start with a correlated three-component fermion system. Its minimal Hamiltonian reads

$$H = \sum_\alpha \int d\mathbf{r} \Psi_\alpha^\dagger(\mathbf{r}) \left(-\frac{\nabla^2}{2m_\alpha} + V_\alpha(\mathbf{r}) + T_\alpha(\mathbf{r}) \right) \Psi_\alpha(\mathbf{r})$$
$$+ \frac{1}{2} \sum_{\alpha \neq \beta} g_{\alpha\beta} \int d\mathbf{r} \Psi_\alpha^\dagger(\mathbf{r}) \Psi_\alpha(\mathbf{r}) \Psi_\beta^\dagger(\mathbf{r}) \Psi_\beta(\mathbf{r}), \quad (1)$$

where $\Psi_\alpha^\dagger(\mathbf{r})$ [$\Psi_\alpha(\mathbf{r})$] is the creation (annihilation) field operator for the α-component particle. α takes three different values, for instance, 1,2,3. m_α is the mass of the α component of the particles. In general, each component can have a different mass. $V_\alpha(\mathbf{r})$ is the lattice potential formed by two counterpropagating laser beams for each space direction, and $T_\alpha(\mathbf{r})$ is the external trapping potential for α-component particles. $g_{\alpha\beta}$ denotes the local interaction between the α and β components. The lattice potential is periodic with the wave vector k_L of the laser beam, for example,

$$V_\alpha(\mathbf{r}) = V_{0\alpha}[\sin^2(k_L x) + \sin^2(k_L y) + \sin^2(k_L z)], \quad (2)$$

where $V_{0\alpha}$ is the amplitude of the lattice potential. It will form an optical lattice with the lattice constant $a = \pi/k_L$. The key feature of the lattice potentials is the component dependence of their amplitudes. These amplitudes are separately tunable for each particle component. Indeed, they depend on the dipole matrix and laser detuning from atomic resonance, which can be different for different atom components. For a sufficiently deep lattice $V_{0\alpha} > E_\alpha = k_L^2/2m_\alpha$, the particle motion is frozen in the minima of the lattice potential, except for a small tunneling to neighboring minima. The particles are effectively confined and move in the lowest band of the lattice.

Using the basis of the Wannier functions of the lowest Bloch band, we expand the field operators of each component as

$$\Psi_\alpha(\mathbf{r}) = \sum_i w_\alpha(\mathbf{r} - \mathbf{R}_i) c_{i\alpha}, \tag{3}$$

where $w_\alpha(\mathbf{r} - \mathbf{R}_i)$ is the Wannier function located around the well minimum i of the lattice potential and $c_{i\alpha}$ is the annihilation operator for α-component particles at the Wannier wave function state $w_\alpha(\mathbf{r} - \mathbf{R}_i)$. After the expansion, within the tight-binding approximation we obtain

$$H = -\sum_{i,j,\alpha} J_{i,j,\alpha} c_{i\alpha}^\dagger c_{j\alpha} + \frac{1}{2} \sum_{\alpha \neq \beta} U_{\alpha\beta} c_{i\alpha}^\dagger c_{i\alpha} c_{i\beta}^\dagger c_{i\beta}, \tag{4}$$

where

$$J_{i,j,\alpha} = -\int d\mathbf{r} \, w_\alpha^*(\mathbf{r} - \mathbf{R}_i) \left(-\frac{\nabla_\mathbf{r}^2}{2m_\alpha} + V_\alpha(\mathbf{r}) \right) w_\alpha(\mathbf{r} - \mathbf{R}_j),$$

$$U_{\alpha\beta} = g_{\alpha\beta} \int d\mathbf{r} |w_\alpha(\mathbf{r} - \mathbf{R}_i)|^2 |w_\beta(\mathbf{r} - \mathbf{R}_i)|^2.$$

When $i = j$, $J_{i,i,\alpha} \equiv \epsilon_\alpha$ is the energy level of the α component. It controls the filling of the α component and can be absorbed into the chemical potential of the α component $\mu_\alpha \equiv \mu + \epsilon_\alpha$, where μ is the common chemical potential of the system. In the tight-binding approximation we also keep the tunneling of particles between the nearest-neighbor minima of the lattice potential $J_\alpha \equiv J_{\langle i,j \rangle, \alpha}$, where $\langle i, j \rangle$ denotes the nearest-neighbor minima i and j. The amplitude J_α is largest in the particle tunneling between the lattice potential minima. We also keep only the local interaction between different components of particles. In Eq. (4) we have also neglected the trapping potential. In general, it generates the site-dependent chemical potential that leads to an inhomogeneity of the ground state. We restrict ourselves here to considering only homogeneous phases. Both the tunneling amplitude J_α and the local interaction strength $U_{\alpha\beta}$ are component dependent. They can be tuned by the depth of the lattice and the recoil energy [19,20,24,25]. In addition, by using the Feshbach resonance, the scattering length can be varied by adjusting external parameters such as the magnetic field [19,20]. As a consequence, the local interaction strength can also be tuned from weak to strong regimes separately from the tunneling rates. In general, we can consider tunneling rate J_α and the local interaction strength $U_{\alpha\beta}$ to be independent model parameters. When all components and lattice potentials are identical, i.e., $J_\alpha = J$ and $U_{\alpha\beta} = U$, the model described by the Hamiltonian in Eq. (4) is essentially the $SU(3)$ symmetry Hubbard model. With a sufficiently large value U/J, the model exhibits the collective Mott transition at commensurate fillings [3]. This Mott transition is characterized by $\Delta N_d = 3$ [3]. The $SU(3)$ symmetry can be broken either by the local interaction [4] or by the tunneling rate [5–7]. Simple symmetry breaking reduces the $SU(3)$ symmetry to $SU(2) \times U(1)$ symmetry [4–7]. In this case, two particle components and their lattice potentials are identical, with the third component being different. In addition to the Mott transition at commensurate fillings, the $SU(2) \times U(1)$ symmetry Hubbard model also exhibits other Mott transitions such as the orbital-selective one at half filling [4–6]. In the orbital-selective Mott insulator, realized in the $SU(2) \times U(1)$ symmetry Hubbard model, there are

two localized components and one delocalized component. It has $N_d = 2$ distinct kinds of doublons, and its transition is characterized by $\Delta N_d = 1$ [4,6]. The other partial localization is the so-called paired Mott insulator, which also occurs at half filling and exhibits localizations of a pair of different components and of the remaining component [4]. Its transition is characterized by $\Delta N_d = 2$. These Mott transitions are always accompanied by $\Delta N_d \neq 0$. The $SU(2)$ symmetry can further be broken by either the tunneling rate or the local interaction. The $SU(2)$ symmetry breaking caused by interaction also induces the Mott transitions at the incommensurate half filling; however, they are still accompanied by $\Delta N_d = 1$ or $\Delta N_d = 2$ [4]. We will show that, in contrast to the symmetry breaking caused by interaction, the $SU(2)$ symmetry breaking caused by the tunneling rate can additionally induce a Mott transition with $\Delta N_d = 0$. Simple symmetry breaking caused by the tunneling rate is realized by allowing one tunneling rate to vanish. This can be achieved by a sufficiently deep lattice potential $V_{0\alpha} \gg E_\alpha$. For instance, $J_1 = J_2 \neq 0$ and $J_3 = 0$ cause $SU(2) \times U(1)$ symmetry breaking, and the obtained Hamiltonian is essentially the three-component FKM [5,6]. In this case, one particle component is immobile while the other two are mobile. The $SU(2)$ symmetry can further be broken by allowing $J_1 \neq J_2$. When $J_1 \neq J_2$, the mobile components can tunnel between the nearest-neighbor sites with different tunneling rates. It is also equivalent to the case where the mobile components have different bare masses. This asymmetry or mass imbalance can be parameterized by $r = J_2/J_1$. The ratio r is tunable by varying the depth of the lattice potentials for the first two components. In this paper we consider the $SU(2) \times U(1)$ symmetry broken Hubbard model with $J_1 \neq J_2$, $J_3 = 0$, and $U_{12} \neq U_{13} = U_{23}$. This model can be referred to as an asymmetric three-component FKM.

The asymmetric three-component FKM has various well-known limiting cases. When $U_{12} = 0$, the model is equivalent to two independent spinless Falicov-Kimball models [26]. At half filling, it exhibits the Mott transition, but always with $\Delta N_d = 1$ [26]. When $U_{13} = U_{23} = 0$, the mobile components are decoupled from the immobile one. The mobile part describes fermion mixtures of mass-imbalanced components [27,28]. It can be modeled by the asymmetric Hubbard model, which exhibits only the Mott transition with $\Delta N_d = 1$ [29]. When $J_1 = J_2$, the model is the three-component FKM, in which Mott transitions with $\Delta N_d = 1, 2, 3$ may occur, depending on the filling and interactions [5,6].

The asymmetric three-component FKM can be realized by loading three-component fermion atoms or fermion mixtures into optical lattices. Such mixtures can be realized by the atomic isotopes ^{6}Li - ^{40}K [30–32], ^{40}K - ^{161}Dy [33,34], ^{6}Li - ^{173}Yb [35,36], and ^{6}Li - ^{167}Er [37]. One component can be changed to an impurity by allowing the corresponding lattice potential to be deep enough. Experiments have already achieved this impurity state [38].

III. MOTT TRANSITIONS

We study the Mott transitions which possibly occur in the asymmetric three-component Falicov-Kimball model with $J_1 \neq J_2$, $J_3 = 0$, and $U_{12} \equiv U \neq U_{13} = U_{23} \equiv U'$. In this model, the first and second components are mobile, while

the third one is immobile. In contrast to the symmetry case with $r = J_2/J_1 = 1$ [5,6], the first and second components are not equivalent. When $r < 1$, the mass of the first component is lighter than that of the second one. The mass asymmetry $r \neq 1$, as we will show later, will induce a swap Mott transition which is not present in the symmetric case. The principal feature of the DMFT is the momentum independence of the self-energy. It is exact in the limit of infinite space dimensions. The Green's function of the mobile components reads

$$G_\alpha(\mathbf{k}, z) = \frac{1}{z - \varepsilon_\alpha(\mathbf{k}) + \mu_\alpha - \Sigma_\alpha(z)}, \qquad (5)$$

where $\alpha = 1, 2$, $\varepsilon_\alpha(\mathbf{k}) = -2J_\alpha \sum_a \cos(k_a r_a)$, and $\Sigma_\alpha(z)$ is the self-energy of the α component. One can see that the third particle component is immobile, and within the DMFT its dynamics can be excluded from the dynamics of mobile components [26,39]. However, its pair occupancy with other components can be finite and trackable within the DMFT [22,26]. The self-energy $\Sigma_\alpha(z)$ is determined from a single impurity embedded in a dynamical mean field medium. Within the two-site DMFT, the dynamical mean field is represented by the bath of a single site coupled to the single impurity [23]. The impurity dynamics can be described by the following Anderson-like Hamiltonian:

$$H_{\text{imp}} = -\sum_{\alpha=1,2} \mu_\alpha n_\alpha - \mu_3 n_3 + U n_1 n_2 + U' \sum_{\alpha=1,2} n_\alpha n_3$$
$$+ \sum_{\alpha=1,2} V_\alpha c_\alpha^\dagger a_\alpha + \text{H.c.} + \sum_{\alpha=1,2} E_\alpha a_\alpha^\dagger a_\alpha, \qquad (6)$$

where $n_\alpha = c_\alpha^\dagger c_\alpha$ is the number operator of the α component. $a_\alpha^\dagger$ (a_α) is the creation (annihilation) operator, which represents a single-site two-component bath of the dynamical mean field. E_α is the energy level of the single-site bath, and V_α is the hybridization of the single-site bath with the impurity. The bath energy level is determined by the self-consistent conditions of the component filling, i.e.,

$$\langle n_\alpha \rangle = \langle n_\alpha^{\text{imp}} \rangle, \qquad (7)$$

where $\langle n_\alpha \rangle$ is the filling of the α component of the original lattice and $\langle n_\alpha^{\text{imp}} \rangle$ is the one determined from the impurity Hamiltonian in Eq. (6). The hybridization V_α is determined by [23]

$$|V_\alpha|^2 = Z_\alpha M_\alpha^{(2)}, \qquad (8)$$

where $Z_\alpha = [1 - \partial \text{Re} \Sigma_\alpha(\omega)/\partial \omega|_{\omega=0}]^{-1}$ is the mass renormalization and $M_\alpha^{(2)}$ is the bare second-order moment of the α component. We also calculate the pair occupancy of the particle components, i.e., $D_{\alpha\beta} = \langle n_\alpha n_\beta \rangle$. $D_{\alpha\beta} \neq 0$ indicates the formation of the doublon of the α and β components. The number of distinct kinds of doublons N_d equals the number of nonvanishing pair occupancies. The two-site DMFT is a simplified impurity solver in which the dynamical mean field of the α component is simplified to be the single-orbital hybridization function $|V_\alpha|^2/(\omega - E_\alpha)$. As a consequence of the simplification, the dynamical self-consistent equations of the DMFT are simplified to the self-consistent conditions of static quantities in Eqs. (7) and (8). The static quantities, such as the component filling, the mass renormalization, and the pair

occupancy, are well reproduced by the two-site DMFT [23]. However, the dynamics of the system is not fully recovered within the two-site DMFT because the local Green's function and the self-energy are not self-consistently determined in the full energy scale [23]. We use the semicircle function for the bare density of states (DOS) of the mobile components

$$\rho_{0\alpha}(\varepsilon) = \frac{2}{\pi J_\alpha^2} \sqrt{J_\alpha^2 - \varepsilon^2}. \qquad (9)$$

We study the half-filling case $\langle n_1 \rangle = \langle n_2 \rangle = \langle n_3 \rangle = 1/2$, where a rich phase diagram of different Mott transitions occurs [4–7]. At half filling $\mu_1 = \mu_2 = (U + U')/2$, and $\mu_3 = U'$. In numerical calculations we take the total tunneling rate $J_1 + J_2 \equiv J$ as the energy unit. Within this energy unit $J_1/J = 1/(r + 1)$, and $J_2/J = r/(r + 1)$. All interactions are measured in units of J. Without loss of generality, we consider the mass asymmetry parameter $0 \leqslant r = J_2/J_1 \leqslant 1$.

First of all, we consider the limiting cases in which one local interaction vanishes. When $U = 0$ and $U' > 0$, the model is reduced to two independent spinless FKMs with different hopping parameters. Each model exhibits a metal-insulator transition at the critical value $U'_{c\alpha} = 2J_\alpha$ [40]. The two-site DMFT also exactly gives these critical values $U'_{c\alpha}$ of the DMFT. This is a benchmark of the two-site DMFT. These metal-insulator transitions are similar to the Mott transition since they are driven by correlations. Although both the mass renormalization and the pair occupancy also vanish in the Mott insulating phase and are formally similar to the ones in the Brinkman-Rice scenario, these metal-insulator transitions are distinct from the standard Mott transition because the metallic phase is a non-Fermi liquid [41,42]. These metal-insulator transitions are similar to the Mott transition in the Hubbard III approximation, in which the local interaction simply separates and repels two Hubbard subbands [43]. However, in contrast to the non-Fermi-liquid artifact of the Hubbard III approximation, the non-Fermi liquid is the nature of the ground state of the FKM. The immobile component appears like a disorder scatterer, and it products a finite lifetime at the Fermi surface [41,42]. This Falicov-Kimball scenario of the Mott-like transition is distinct from the DMFT scenario of the Mott transition in the Hubbard model and its simplified version, the Brinkman-Rice scenario. Within the Brinkman-Rice scenario, $\text{Im}\Sigma(\omega)$ at $\omega = 0$ vanishes, while in the Falicov-Kimball scenario it is finite. However, the dynamics features of the Falicov-Kimball scenario are not well reproduced by the two-site DMFT. In Fig. 2 we plot the spectral density of the mobile components when $U = 0$. Because we use the semicircle bare DOS in Eq. (9), the spectral density exhibits the renormalized energy bands only along the high-symmetry line with the value $\varepsilon_{\mathbf{k}}$. Within the two-site DMFT, the Falicov-Kimball interaction U' produces an isolated subband near the Fermi energy in the gap between two Hubbard-like subbands. This isolated subband is clearly displayed at the Fermi energy and is suppressed away from the Fermi energy. With increasing U', the isolated subband shrinks and disappears at the metal-insulator transition. However, the exact solution of the DMFT for the Falicov-Kimball model shows a pseudogap instead of the isolated subband [26].
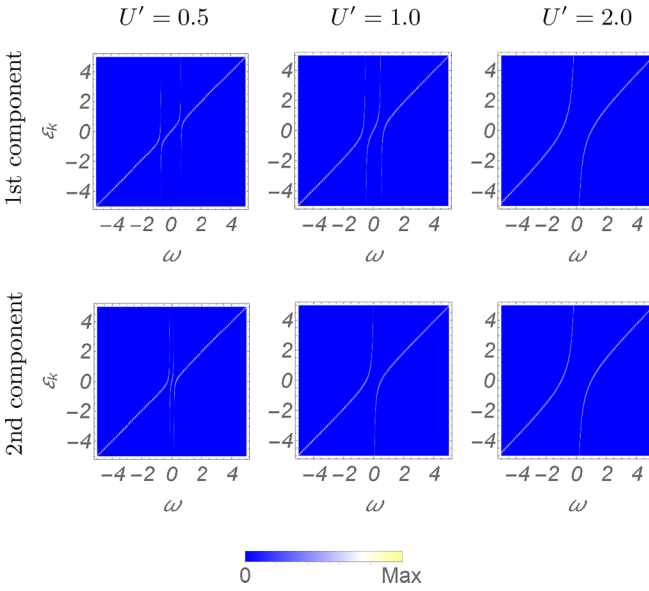
FIG. 2. The spectral density of the mobile components in the color density plot. The first (second) row presents the spectral density of the first (second) component for various values of U' ($U = 0$).

FIG. 4. The spectral density of the mobile components in the color density plot. The first (second) row presents the spectral density of the first (second) component for various values of U ($U' = 0$).

In Fig. 3 we plot the pair occupancies and the mass renormalizations as a function of U', when $U = 0$. Because the first and second components are independent, at half filling their pair occupancy D_{12} never vanishes. However, their pair occupancies for the third component (D_{13}, D_{23}) may vanish, depending on the value of the local interaction U', as shown in Fig. 3. For sufficiently large local interaction U', all particle components are localized; however, only the pair occupancies D_{13} and D_{23} vanish because $U = 0$ allows the first two components to occupy at the same lattice site, although they are localized. This insulating state is characterized by $N_d = 1$ and is distinguishable from the collective Mott insulator, where all pair occupancies are suppressed. For intermediate values
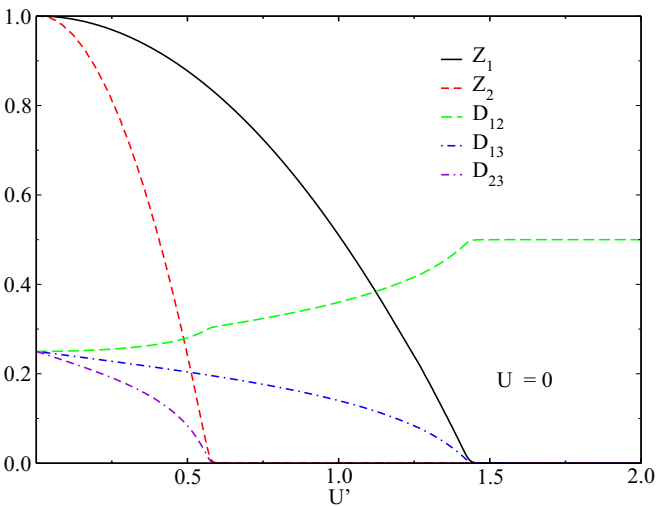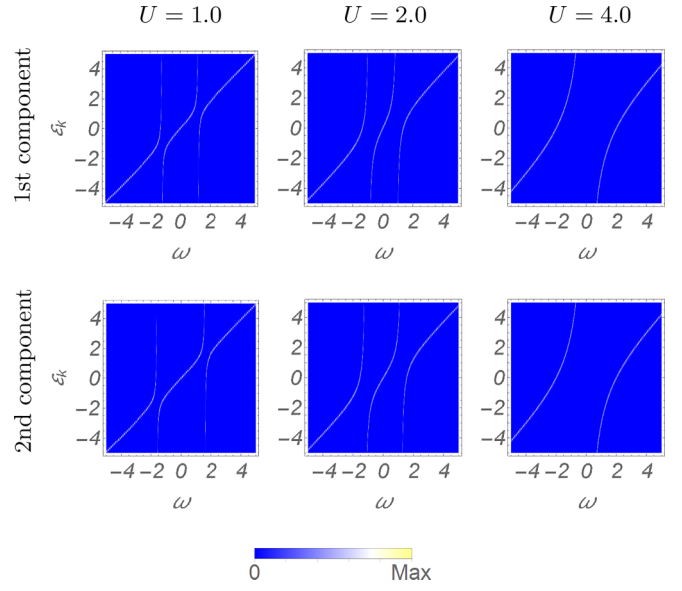

FIG. 3. The pair occupancies $D_{\alpha\beta}$ and the mass renormalization Z_α as a function of U' ($U = 0$). The mass asymmetry parameter $r = 0.4$.

$U'_{c2} < U' < U'_{c1}$, the previously suppressed pair occupancy, D_{13}, becomes finite. This state is partially localized because the lighter component (i.e., the component with the larger hopping parameter) can be mobile in this regime. It reflects the finite mass renormalization of the lighter component. In the intermediate regime of the local interaction, the Mott insulator is characterized by $N_d = 2$. When the local interactions are weak, $U' < U'_{c2}$, both heavier and lighter components become delocalized. The ground state is a metal, which is characterized by $N_d = 3$. However, this metallic state is a non-Fermi liquid. In the limiting case $U = 0$, the Mott transitions always occur with $\Delta N_d = 1$.

The other limiting case is $U' = 0$, $U > 0$. The considered model is reduced to the standard asymmetric Hubbard model, which is well studied [29]. Within the DMFT the Mott transition occurs at the critical value $U_c = J_1 + J_2 + (J_1^2 + J_2^2 + 14 J_1 J_2)^{1/2}$ [29]. The two-site DMFT also reproduces well this critical value. In contrast to the Falicov-Kimball scenario, in this limiting case, the Mott transition can simply be described by the Brinkman-Rice scenario. In Fig. 4 we plot the spectral density of the mobile components for various values of U at fixed $U' = 0$. The local interaction between the mobile components U also produces a subband in the gap between the two Hubbard subbands. However, in contrast to the limiting case $U = 0$, the inside-gap subband is extended to the band edges, especially when the system is close to the metal-insulator transition, and completely disappears in the insulating phase. This subband mimics the one generated by the Kondo resonance, which also appears before the metal-insulator transition and completely disappears in the insulating phase [22]. This behavior of the subband also distinguishes between the Falicov-Kimball and Brinkman-Rice scenarios, although the full dynamics of the subband is displayed only in the full DMFT. However, the static quantities, such as the filling and the mass renormalization, are
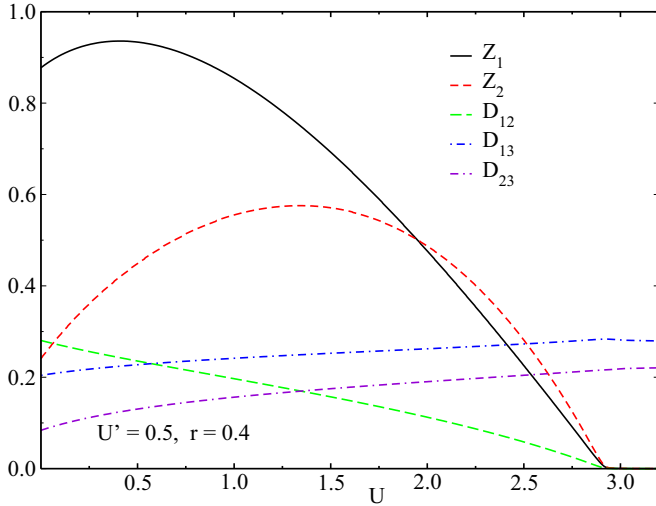
FIG. 5. The pair occupancies $D_{\alpha\beta}$ and the mass renormalization Z_α as a function of U at fixed $U' = 0.5$ and $r = 0.4$.

FIG. 6. The pair occupancies $D_{\alpha\beta}$ and the mass renormalization Z_α as a function of U at fixed $U' = 1.0$ and $r = 0.4$.

self-consistently determined in the two-site DMFT, and we can also use them to monitor the Mott transition. The mass renormalizations Z_1 and Z_2 and the pair occupancy D_{12} clearly vanish at the Mott transition [29] (see similar behavior in Fig. 5). In contrast to the asymmetric two-component Hubbard model [29], $U' = 0$ allows the third component to occupy the lattice sites which are already occupied by the first or second component. Therefore, the pair occupancies D_{13} and D_{23} never vanish. One may naively expect the heavier component to be more affected by the local interaction, and it would be more strongly renormalized by correlations. However, the DMFT result reveals the opposite [29]. The effective mass of the lighter component is more strongly reduced by the local interaction $Z_2 < Z_1$. However, as we will see later, weak local interaction U' will remove this anomalous behavior near the transition point. In the strong interaction regime with $U > U_c$, the pair occupancy D_{12} vanishes, and the Mott insulator is characterized by $N_d = 2$. In the opposite regime with $U < U_c$, all pair occupancies are finite, and this metallic state is characterized by $N_d = 3$. The Mott transition, therefore, is characterized by $\Delta N_d = 1$.

When both local interactions U and U' are finite, one may expect competition between the Brinkman-Rice and the Falicov-Kimball scenarios of the Mott transition. We analyze the Mott transition driven by the local interaction between the mobile components U at a different fixed local interaction U' and mass asymmetry $r < 1$. From the impurity Hamiltonian in Eq. (6), we can see that n_3 is a good quantum number. It can take two values: 0 or 1. The local Green's function of the α component, therefore, reads [5]

$$G_\alpha(\omega) = \frac{1 - \langle n_3 \rangle}{\mathcal{G}_\alpha^{-1}(\omega) - \Delta_\alpha^{(0)}(\omega)} + \frac{\langle n_3 \rangle}{\mathcal{G}_\alpha^{-1}(\omega) - \Delta_\alpha^{(1)}(\omega) - U'}, \tag{10}$$

where $\mathcal{G}_\alpha(\omega)$ is a Green's function which represents the effective mean field medium surrounding the single α-component site and $\Delta_\alpha^{(n_3)}(\omega)$ is the self-energy of the α component due to the local interaction U in the Fock space sectors with
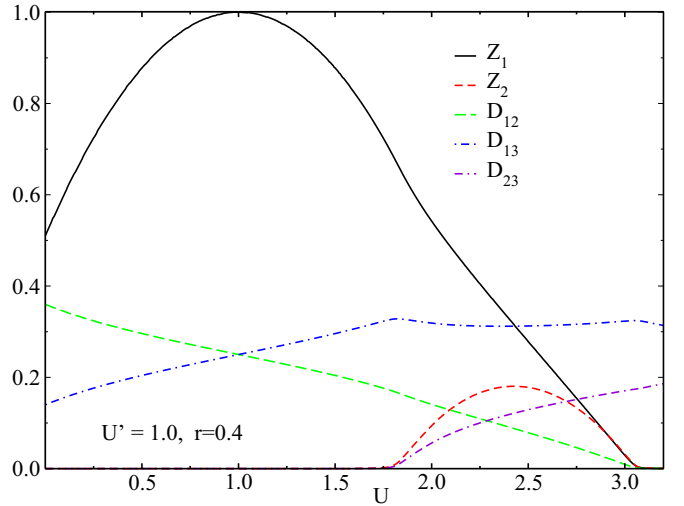
$n_3 = 0, 1$. When U is large, the self-energy $\Delta_\alpha^{(n_3)}(\omega)$ is dominant over the U' term, and the Mott transition belongs to the Brinkman-Rice scenario. In contrast, when U' is large, the U' term is dominant over the self-energy $\Delta_\alpha^{(n_3)}(\omega)$, and the Falicov-Kimball scenario of the Mott-like transition is realized. As a consequence of that competition, for finite interactions, there are four distinct regions of U' where different scenarios of the Mott transitions are realized. However, within the two-site DMFT, both $\mathcal{G}_\alpha(\omega)$ and $\Delta_\alpha^{(n_3)}(\omega)$ are simplified and not self-consistently determined. Therefore, we mainly analyze the scenario of the metal-insulator transition through the static quantities.

(1) $U' < U'_{c2}$. In this value range of U', we observe only one Mott transition driven by U, as shown in Fig. 5. This Mott transition is similar to the one in the limiting case $U' = 0$ and is also characterized by $\Delta N_d = 1$. However, in contrast to the limiting case, close to the transition point, the anomalous behavior of the mass renormalizations $Z_2 < Z_1$ stops, and the lighter component is more renormalized than the heavier one. The finite value of U' also increases the critical value of U, where the Mott transition occurs. This indicates that in the presence of the third component, the weak local interactions of the third component with the other components try to prevent the Mott transition until the local interaction U suppresses the mobility of the mobile components. Note that due to the mass asymmetry $r < 1$, $D_{13} \neq D_{23}$.

(2) $U'_{c2} < U' < U'_{c1}$. In this value region of U', there are two Mott transitions driven by U at critical values U_{c1} and U_{c2}, as shown in Fig. 6. In the weak interaction regime, $U < U_{c1}$, the heavier component is localized, while the lighter component is still mobile. This regime is similar to the limiting case $U = 0$. The pair occupancy D_{23} vanishes due to the prevention of the local interaction U' at small values of J_2. However, the local interaction U' still cannot suppress the pair occupancy D_{13} because $J_1 > J_2$. This Mott insulator is characterized by $N_d = 2$. With a further increase in the local interaction, $U_{c1} < U < U_{c2}$, the pair occupancy D_{23} becomes finite. In this range of the local interaction U, it only renormalizes the masses of
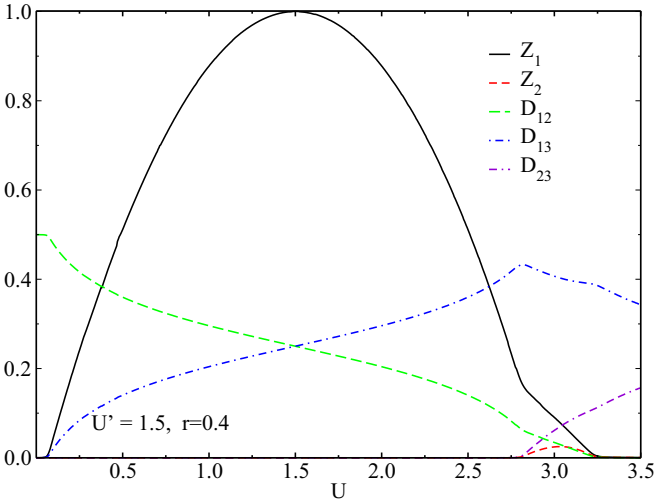
FIG. 7. The pair occupancies $D_{\alpha\beta}$ and the mass renormalization Z_α as a function of U at fixed $U' = 1.5$ and $r = 0.4$.

FIG. 8. The pair occupancies $D_{\alpha\beta}$ and the mass renormalization Z_α as a function of U at fixed $U' = 2.5$ and $r = 0.4$.

the mobile components. The ground state is metallic. When the local interaction increases, $U > U_{c2}$, it is strong enough to suppress the mobility of mobile components. The pair occupancy D_{12} vanishes like in the two-component Hubbard model [23,40]. This Mott transition is still characterized by $\Delta N_d = 1$. One can see that two Mott transitions have different origins. In the first one, the pair occupancy D_{23} vanishes due to the Falicov-Kimball mechanism, while in the second one D_{12} vanishes by the Brinkman-Rice scenario.

(3) $U'_{c2} < U' < U'_t$. Here we have introduced a certain value U'_t of the local interaction U' which separates distinct phases of the system. As we will see later, U'_t is the value of the local interaction U' at a tricritical point where the metal, Mott insulator, and partial localization coexist. In Fig. 7 we plot the pair occupancies $D_{\alpha\beta}$ and the mass renormalization Z_α as function of U in this regime. Since $U' > U'_{c2}$, even at $U = 0$ the ground state is the Mott insulator. This Mott insulator occurs for weak interactions U because the local interaction U' prevents the pair occupancies of the mobile and immobile components like in the FKM [26]. However, the weak interaction U still allows the mobile components to occupy the same lattice sites. Therefore, the Mott insulator is characterized by $N_d = 1$. With a further increase in U, the localization of the lighter component stops, while the heavier component is still localized. In this regime, the local interaction U takes its effect over U'. As a consequence, the lighter component recovers its Fermi-liquid behaviors due to its mobility, while the heavier component cannot do that due to its localization. The partial localization is characterized by $N_d = 2$. When the local interaction U becomes stronger, the heavier component recovers its Fermi-liquid behaviors too, and it becomes mobile, as shown in Fig. 7. The ground state is metallic, and it is characterized by $N_d = 3$. However, when the local interaction U_{12} is strong enough, it suppresses the pair occupancy of the mobile components, like in the standard two-component Hubbard model. The ground state is fully Mott insulating state, which is characterized by $N_d = 2$. So far, in this regime, all Mott transitions driven by the local interaction U are characterized by $\Delta N_d = 1$.
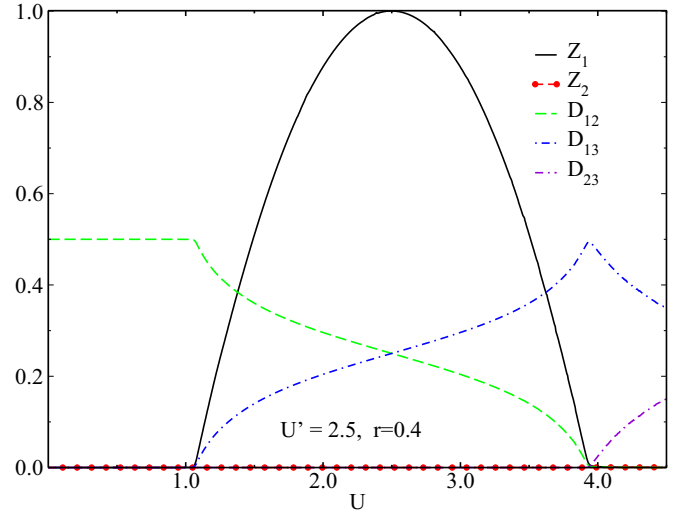
(4) $U' > U'_t$. In contrast to the previous regime, when the local interaction U' is strong enough, the local interaction U between the mobile components cannot recover the mobility of the heavier component. As a consequence, the heavier component is always localized, and its mass renormalization vanishes, independent of the value of U, as shown in Fig. 8. However, the local interaction U can recover the metallic behaviors of the lighter component when U is dominant over U'. In Fig. 8, we can see that the lighter component is mobile in the intermediate regime of U. This partial localization is characterized by $N_d = 2$. In the weak regime of U, the effect of U' dominates over U, and this leads to the localization of the lighter component. The ground state of the system has $N_d = 1$. However, in the strong regime of U, both lighter and heavier components become localized, like in the standard two-component Hubbard model [29]. In this regime, since U is dominant over U', the pair occupancies D_{13} and D_{23} are not suppressed. Therefore, the localized state is also characterized by $N_d = 2$. As a consequence, the transition from the intermediate to strong regimes has the same $N_d = 2$. Across this transition, the lighter and immobile components are swapped with each other. The transition is characterized by $\Delta N_d = 0$. This is the swap Mott transition and is absent in the symmetric case with $r = 1$ [5,6]. In the symmetric case with $r = 1$, $D_{13} = D_{23}$, and the partial localization is absent. These phase transitions can also be seen in the spectral density behaviors. Figure 9 shows the spectral density of the mobile components for various values of U with fixed $U' > U'_t$. In this regime, the spectral density of the heavier (second) component always exhibits a gap at half filling. This property is consistent with the localization of the heavier component. The weak and intermediate interactions U cannot recover the localization of the heavier component due to the strong interaction U'. However, the intermediate interactions U induce a subband near the Fermi energy and recover the metallic behavior of the lighter (first) component. In this regime, the doublon may be formed by the lighter component with the heavier component and with the immobile component. Thus, the number of distinct
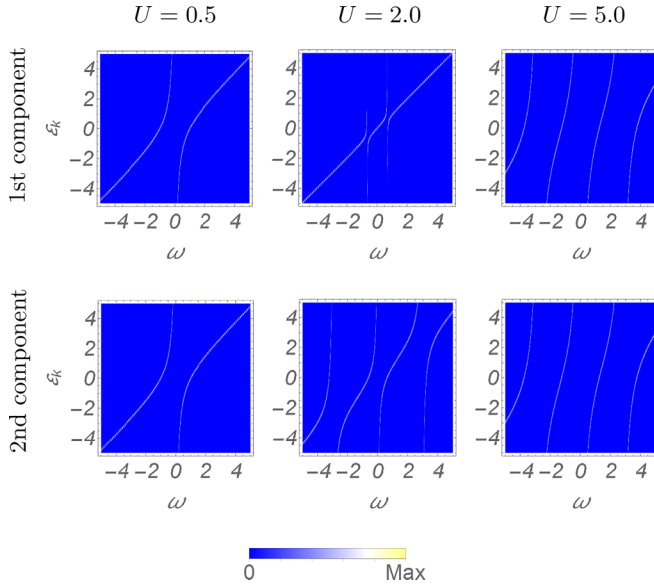
FIG. 9. The spectral density of the mobile components in the color density plot. The first (second) row presents the spectral density of the first (second) component for various values of U at fixed $U' = 2.5$.

kinds of doublons $N_d = 2$. When the interaction U is strong, it again suppresses the mobility of the lighter component. It also suppresses the doublon formation of the lighter and heavier components. As a consequence, $N_d = 2$.

We summarize the phase transitions we found in the phase diagram in Fig. 10. The insulating phase labeled (A) is established by the Brinkman-Rice scenario, in which the local interaction U is dominant over the local interaction U' and suppresses the pair occupancy of the two mobile components. As a consequence, in this phase two distinct kinds of doublons are formed by the third component with mobile components,
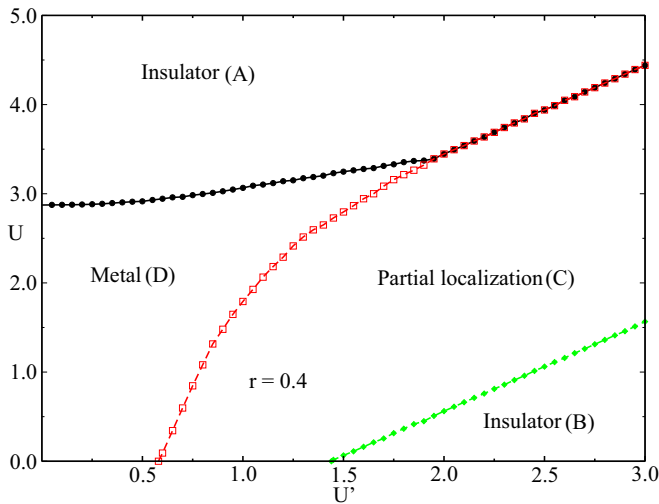

FIG. 10. Phase diagram at half filling $\langle n_1 \rangle = \langle n_2 \rangle = \langle n_3 \rangle = 1/2$. In the insulator labeled (A) $N_d = 2$, in the insulator labeled (B) $N_d = 1$, in the partial localization labeled (C) $N_d = 2$, and in the metal labeled (D) $N_d = 3$.

and $N_d = 2$. In contrast, the insulating phase labeled (B) occurs within the Falicov-Kimball scenario, where the local interaction U' is dominant over the local interaction U and suppresses the pair occupancies between the third component and mobile components. Therefore, in this phase $N_d = 1$. Between these two insulating phases, a metallic phase with $N_d = 3$ and a partially localized phase with $N_d = 2$ occur. The metallic phase must terminate at a tricritical point, where the Mott insulator, partial localization, and metal coexist. It cannot naturally exist when both interactions U and U' are strong. The metallic phase may be a mixture of Fermi and non-Fermi liquids because in one limit, $U' = 0$, it is a Fermi liquid but in the other limit, $U = 0$, it is a non-Fermi liquid. It is similar to the weakly Anderson localization, which was found in the two-component FKM [42]. However, the two-site DMFT cannot detect the mixture, and we leave the nature of the metallic phase for further study. The partially localized phase labeled (C) is characterized by the localization of the heavy mobile component, but it still allows the mobility of the light component. As a consequence, two distinct kinds of doublons are formed by the light components and the other components. The competition between the Brinkman-Rice scenario and the Falicov-Kimball scenario, together with the asymmetry of the two mobile components, gives rise to the partially localized phase. This phase is absent in the symmetric case with $r = 1$. There are two ways for the phase transition from the partial localization (phase C) to the Mott insulator (phase A) to occur. One transition occurs via the metallic phase, and the other is the direct phase transition from the partial localization to the Mott insulator. The latter phase transition is a swap Mott transition with $\Delta N_d = 0$. The asymmetric three-component FKM may be realized by loading ultracold atoms into an optical lattice. It is a challenge to detect the swap Mott transition by monitoring the doublon formation.

IV. CONCLUSION

We studied Mott transitions in the asymmetric three-component FKM by applying the two-site DMFT. The asymmetric three-component FKM was obtained from the symmetry breaking of the $SU(3)$ Hubbard model by both hopping and local interactions. The Mott transitions are characterized by the change in the number of distinct kinds of doublons. At half filling, we found different Mott insulating phases. In addition to the insulating phases established by the Brinkman-Rice and the Falicov-Kimball scenarios, we found a partially localized phase in which the heavy mobile component becomes localized, while the light component is still able to move in the lattice. A swap Mott transition, in which both phases have the same number of distinct kinds of doublons, was observed. Across the swap Mott transition, the light and immobile components are swapped with each other. Our results may shed some light on the localization in multicomponent correlated systems, in which different localization mechanisms may take action. In particular, the exotic fractionalized state may be relevant to the localization [8,9]. Our results are also relevant to studies of localization in ultracold atomic mixtures [30–37]. The proposed model may serve as a prototype for the implementation of the mass imbalance in optical lattices. It would be interesting to see an

experimental confirmation of the swap Mott transition. However, the dynamical properties of the system are not fully taken into account by the two-site DMFT. We leave the dynamical problem for further study.

[1] N. F. Mott, *Metal-Insulator Transitions*, 2nd ed. (Taylor and Francis, London, 1990).

[2] W. F. Brinkman and T. M. Rice, Application of Gutzwiller's variational method to the metal-insulator transition, Phys. Rev. B **2**, 4302 (1970).

[3] E. V. Gorelik and N. Blümer, Mott transitions in ternary flavor mixtures of ultracold fermions on optical lattices, Phys. Rev. A **80**, 051602(R) (2009).

[4] K. Inaba, S. Y. Miyatake, and S. I. Suga, Mott transitions of three-component fermionic atoms with repulsive interaction in optical lattices, Phys. Rev. A **82**, 051602(R) (2010).

[5] D.-B. Nguyen and M.-T. Tran, Mott transitions in three-component Falicov-Kimball model, Phys. Rev. B **87**, 045125 (2013).

[6] D.-A. Le and M.-T. Tran, Mott transitions in a three-component Falicov-Kimball model: A slave boson mean-field study, Phys. Rev. B **91**, 195144 (2015).

[7] D.-B. Nguyen, D.-K. Phung, V.-N. Phan, and M.-T. Tran, Metal-insulator transition induced by mass imbalance in a three-component Hubbard model, Phys. Rev. B **91**, 115140 (2015).

[8] M. Hohenadler and F. F. Assaad, Fractionalized metal in a Falicov-Kimball model, Phys. Rev. Lett. **121**, 086601 (2018).

[9] M.-T. Tran, Fractionalized long-range ordered state in a Falicov-Kimball model, Phys. Rev. B **99**, 165104 (2019).

[10] R. Jördens, N. Strohmaier, K. Günter, H. Moritz, and I. Esslinger, A Mott insulator of fermionic atoms in an optical lattice, Nature (London) **455**, 204 (2008).

[11] U. Schneider, L. Hackermüller, S. Will, T. Best, I. Bloch, T. A. Costi, R. W. Helmes, D. Rasch, and A. Rosch, Metallic and insulating phases of repulsively interacting fermions in a 3D optical lattice, Science **322**, 1520 (2008).

[12] G. Zwicknagl and P. Fulde, The dual nature of 5f electrons and the origin of heavy fermions in U compounds, J. Phys.: Condens. Matter **15**, S1911 (2003).

[13] D. V. Efremov, N. Hasselmann, E. Runge, P. Fulde, and G. Zwicknagl, Dual nature of $5f$ electrons: Effect of intra-atomic correlations on hopping anisotropies, Phys. Rev. B **69**, 115114 (2004).

[14] E. Runge, P. Fulde, D. V. Efremov, N. Hasselmann, and G. Zwicknagl, Approximative treatment of $5f$-systems with partial localization due to intra-atomic correlations, Phys. Rev. B **69**, 155110 (2004).

[15] V. I. Anisimov, I. A. Nekrasov, D. E. Kondakov, T. M. Rice, and M. Sigrist, Orbital-selective Mott-insulator transition in $Ca_{2-x}Sr_xRuO_4$, Eur. Phys. J. B **25**, 191 (2002).

[16] A. Koga, N. Kawakami, T. M. Rice, and M. Sigrist, Orbital-selective Mott transitions in the degenerate Hubbard model, Phys. Rev. Lett. **92**, 216402 (2004).

[17] A. Liebsch, Single Mott transition in the multiorbital Hubbard model, Phys. Rev. B **70**, 165103 (2004).

[18] L. de'Medici, A. Georges, and S. Biermann, Orbital-selective Mott transition in multiband systems: Slave-spin representation and dynamical mean-field theory, Phys. Rev. B **72**, 205124 (2005).

[19] M. Lewenstein, A. Sanpera, V. Ahufinger, B. Damski, A. S. De, and U. Sen, Ultracold atomic gases in optical lattices: Mimicking condensed matter physics and beyond, Adv. Phys. **56**, 243 (2007).

[20] I. Bloch, J. Dalibard, and W. Zwerger, Many-body physics with ultracold gases, Rev. Mod. Phys. **80**, 885 (2008).

[21] W. Metzner and D. Vollhardt, Correlated lattice fermions in $d = \infty$ dimensions, Phys. Rev. Lett. **62**, 324 (1989).

[22] A. Georges, G. Kotliar, W. Krauth, and M. J. Rozenberg, Dynamical mean-field theory of strongly correlated fermion systems and the limit of infinite dimensions, Rev. Mod. Phys. **68**, 13 (1996).

[23] M. Potthoff, Two-site dynamical mean-field theory, Phys. Rev. B **64**, 165114 (2001).

[24] W. Zwerger, Mott–Hubbard transition of cold atoms in optical lattices, J. Opt. B **5**, S9 (2003).

[25] M. Dalmonte, K. Dieckmann, T. Roscilde, C. Hartl, A. E. Feiguin, U. Schollwöck, and F. Heidrich-Meisner, Dimer, trimer, and Fulde-Ferrell-Larkin-Ovchinnikov liquids in mass- and spin-imbalanced trapped binary mixtures in one dimension, Phys. Rev. A **85**, 063608 (2012).

[26] J. K. Freericks and V. Zlatic, Exact dynamical mean-field theory of the Falicov-Kimball model, Rev. Mod. Phys. **75**, 1333 (2003).

[27] P. Zdybel and P. Jakubczyk, Effective potential and quantum criticality for imbalanced Fermi mixtures, J. Phys.: Condens. Matter **30**, 305604 (2018).

[28] P. Chankowski and J. Wojtkiewicz, On the ground-state energy of a mixture of two different oppositely polarized fermionic gases, Acta Phys. Pol. B **53**, 1-A3 (2022).

[29] T. L. Dao, M. Ferrero, P. S. Cornaglia, and M. Capone, Mott transition of fermionic mixtures with mass imbalance in optical lattices, Phys. Rev. A **85**, 013606 (2012).

[30] E. Wille, F. M. Spiegelhalder, G. Kerner, D. Naik, A. Trenkwalder, G. Hendl, F. Schreck, R. Grimm, T. G. Tiecke, J. T. M. Walraven, S. J. J. M. F. Kokkelmans, E. Tiesinga, and P. S. Julienne, Exploring an ultracold Fermi-Fermi mixture: Interspecies Feshbach resonances and scattering properties of ^{6}Li and ^{40}K, Phys. Rev. Lett. **100**, 053201 (2008).

[31] A.-C. Voigt, M. Taglieber, L. Costa, T. Aoki, W. Wieser, T. W. Hänsch, and K. Dieckmann, Ultracold heteronuclear Fermi-Fermi molecules, Phys. Rev. Lett. **102**, 020405 (2009).

[32] L. Costa, J. Brachmann, A.-C. Voigt, C. Hahn, M. Taglieber, T. W. Hänsch, and K. Dieckmann, s-wave interaction in a two-species Fermi-Fermi mixture at a narrow Feshbach resonance, Phys. Rev. Lett. **105**, 123201 (2010).

[33] C. Ravensbergen, V. Corre, E. Soave, M. Kreyer, E. Kirilov, and R. Grimm, Production of a degenerate Fermi-Fermi mixture

of dysprosium and potassium atoms, Phys. Rev. A **98**, 063624 (2018).

[34] C. Ravensbergen, E. Soave, V. Corre, M. Kreyer, B. Huang, E. Kirilov, and R. Grimm, Resonantly interacting Fermi-Fermi mixture of ^{161}Dy and ^{40}K, Phys. Rev. Lett. **124**, 203402 (2020).

[35] H. Hara, Y. Takasu, Y. Yamaoka, J. M. Doyle, and Y. Takahashi, Quantum degenerate mixtures of alkali and alkaline-earth-like atoms, Phys. Rev. Lett. **106**, 205304 (2011).

[36] A. Green, H. Li, J. H. S. Toh, X. Tang, K. C. McCormick, M. Li, E. Tiesinga, S. Kotochigova, and S. Gupta, Feshbach resonances in p-wave three-body recombination within Fermi-Fermi mixtures of open-shell ^{6}Li and closed-shell ^{173}Yb atoms, Phys. Rev. X **10**, 031037 (2020).

[37] F. Schäfer, Y. Haruna, and Y. Takahashi, Observation of Feshbach resonances in an ^{167}Er $-$ ^{6}Li Fermi–Fermi mixture, J. Phys. Soc. Jpn. **92**, 054301 (2023).

[38] H. Hara, H. Konishi, S. Nakajima, Y. Takasu, and Y. Takahashi Y, A three-dimensional optical lattice of ytterbium and lithium atomic gas mixture, J. Phys. Soc. Jpn. **83**, 014003 (2014).

[39] U. Brandt and M. P. Urbanek, The f-electron spectrum of the spinless Falicov-Kimball model in large dimensions, Z. Phys. B **89**, 297 (1992).

[40] R. Bulla and M. Potthoff, "Linearized" dynamical mean-field theory for the Mott-Hubbard transition, Eur. Phys. J. B **13**, 257 (2000).

[41] Q. Si, G. Kotliar, and A. Georges, Falicov-Kimball model and the breaking of Fermi-liquid theory in infinite dimensions, Phys. Rev. B **46**, 1261 (1992).

[42] A. E. Antipov, Y. Javanmard, P. Ribeiro, and S. Kirchner, Interaction-tuned Anderson versus Mott localization, Phys. Rev. Lett. **117**, 146601 (2016).

[43] R. Hubbard, Electron correlations in narrow energy bands III. An improved solution, Proc. R. Soc. London, Ser. A **281**, 401 (1964).